In-vivo imaging results with ultrasound tomography: Report on an ongoing study at the Karmanos Cancer Institute

Nebojsa Duric, PhD, Peter Littrup, MD, Priti Chandiwala-Mody, Cuiping Li, PhD, Steven Schmidt, Lukasz Myc, Olsi Rama, Lisa Bey-Knight, Jessica Lupinacci, Bryan Ranger, Amy Szczepanski, Erik West.

Karmanos Cancer Institute, 110 East Warren, Hudson-Webber Cancer Research Center, Room 4246, Detroit MI 48201

ABSTRACT

Our laboratory has focused on the development of ultrasound tomography (UST) for breast imaging. To that end we have been developing and testing a clinical prototype in the Karmanos Cancer Institute's (KCI) breast center. The development of our prototype has been guided by clinical feedback from data accumulated from over 300 patients recruited over the last 4 years. Our techniques generate whole breast reflection images as well as images of the acoustic parameters of sound speed and attenuation. The combination of these images reveals major breast anatomy, including fat, parenchyma, fibrous stroma and masses. Fusion imaging, utilizing thresholding, is shown to visualize mass characterization and facilitates separation of cancer from benign masses. These results indicate that operator-independent whole-breast imaging and the detection and characterization of cancerous breast masses are feasible using acoustic tomography techniques.

Analyses of the prototype images suggests that we can detect the variety of mass attributes noted by current ultrasound-BIRADS criteria, such as mass shape, acoustic mass properties and architecture of the tumor environment. These attributes help quantify current BIRADS criteria (e.g. "shadowing" or high attenuation) and provide greater possibilities for defining a unique signature of cancer. The potential for UST to detect and characterize breast masses was quantified using UST measurements of 86 masses from the most recent cohort of patients imaged with the latest version of our prototype. Our preliminary results suggest that the development of a formal predictive model, in support of larger future trials, is warranted.

Keywords: Breast imaging, breast masses, image fusion, ultrasound tomography

1. INTRODUCTION

Mammography screening has been shown to reduce the mortality rate in multiple screening trials[1]. However, diagnostic mammography generates many abnormal findings not related to cancer that leads to additional, costly imaging procedures and biopsies[2-5]. Magnetic Resonance Imaging (MRI) is making increasing inroads into diagnostic breast imaging by virtue of its high sensitivity and operator independence. Consequently, for high-risk women, MRI is now viewed as the highest standard for breast cancer early detection and screening[6-7]. However, it can have a high false positive rate, requires contrast injection and the exams can be both long and costly.

Recent studies have demonstrated the effectiveness of ultrasound imaging in detecting breast cancer[8-10], particularly for women with dense breasts. The ongoing ACRIN 6666 study, funded by the Avon Foundation and the NCI, represents a definitive trial evaluating the potential of ultrasound as a screening tool[9]. The latest reports have shown the potential to screen for small breast masses otherwise missed by mammography[10]. Despite these successes, ultrasound is unlikely to fill the gap between the cost effectiveness of mammography and the imaging quality of MRI for the following reasons:

(i) The added cancers found by ultrasound are offset by an increased burden of false positives[10], indicating that characterization of small masses by conventional ultrasound is limited. (ii) The operator-dependent nature of ultrasound will prevent uniform replication of results. (iii) The associated small-aperture-imaging leads to long exam times and the need to "stitch" the localized images into a whole breast view. Addressing the problems of current ultrasound to give it the volumetric image acquisition and operator independence of MRI would be, therefore, a major advance toward a clinically successful screening option.

Historically, two general approaches have been used to advance operator-independent sonography. One approach has been based on improving the current ultrasound devices and techniques which rely on reflection (or B-mode) imaging while the second utilizes transmission imaging to characterize masses.

Stavros et al proposed that analysis of mass margins, shape and echo-properties, based on conventional, *reflection* ultrasound images, could lead to highly accurate differentiation of benign masses from cancer[11]. These observations led to the development of the "Stavros Criteria" which evolved into the Breast Imaging Reporting and Data System (BIRADS) for ultrasound. In order to implement this analysis into a screening scenario, attempts have been made to construct operator-independent scanners that image the whole breast (see Norton and Linzer for an early example[12]). The only commercial device to achieve any clinical acceptance thus far has been that of U-Systems[13].

In 1976, Greenleaf et al made the seminal observation that acoustic measurements made with transmission ultrasound could be used to characterize breast tissue[14]. On the basis of these studies, they concluded that using the imaging parameters of sound speed and attenuation (henceforth the *Greenleaf* criteria) could help differentiate benign masses from cancer. As a direct result of this and other similar studies, a number of investigators developed operator-independent ultrasound scanners, based on the principles of ultrasound tomography, in an attempt to measure the *Greenleaf* criteria with in-vivo scans.[15-21]. Examples include the work of Carson et al (U. Michigan)[15], Andre et al (UCSD)[16], Johnson et al (TechniScan Medical Systems)[17], Marmarelis et al (USC)[18], Liu and Waag (U. Rochester)[19] and Duric and Littrup et al (KCI)[20-21].

Our laboratory has focused on the development of ultrasound tomography for breast imaging. To that end we have been developing and testing a clinical prototype in KCI's breast center. We have demonstrated the feasibility of breast cancer detection with ultrasound tomography and set the stage for a variety of clinical research projects aimed at the life cycle of breast cancer, from risk assessment[22-23] to detection[24] to therapy monitoring[25]. The continuing development of the prototype and its associated UST methodology have been guided by clinical feedback from these studies and has led to significant improvements in imaging performance leading to greater clinical relevance. This paper presents the most recent imaging capabilities of the UST methodology that were enabled by these improvements.

2. METHODS

The studies described in this paper were carried out with an updated prototype that was used to image over 100 patients using improved reconstruction algorithms.

The prototype:

The prototype is described fully in pervious publications. Here we summarize the basic operating characteristics.

- With data acquisition time of 0.03s per slice, the prototype scans patients without motion artifacts. To the best of our knowledge, this is the fastest ultrasound tomographic scanner collecting clinical data.
- Operating at a central frequency of 2 MHz, where signal scattering is relatively low, consistent penetration of the whole breast is assured.
- The scanner has an integrated transducer array that yields simultaneous data for reconstructions of reflectivity, attenuation, and sound speed parameters of tissue throughout the breast. This capability yields automatic image registration, facilitating image fusion, which greatly aids clinical analysis.
- The prototype has demonstrated fully operator-independent breast exams.
- A flexible table-top made out of sail-cloth is designed to take advantage of the patient's weight and allow for exposure of the chest wall into the imaging tank, leading to chest wall access (Fig 1).

- The components used to construct the prototype are cost-effective and reflect the inherently inexpensive nature of ultrasound technology.

The most recent upgrade of the prototype was completed in November 2007. The improved prototype was used to study over 100 patients.

Patient recruitment and data collection

All imaging procedures were performed under an Institutional Review Board-approved protocol, in compliance with the Health Insurance Portability and Accountability Act, with informed consent obtained from all patients. Patients were selected if they exhibited a suspicious mass after mammography and/or follow-up ultrasound. The ultrasound tomography exam was scheduled after these conventional examinations, but before biopsy. A typical whole breast exam takes about 1 minute to perform. The total time the patient spends in the exam room is about 5 minutes. A patient exam begins with the patient lying prone on the scanner table. The table consists of flexible sailcloth, which contours to the patient's body, thereby increasing access to the axilla regions of the breast and increasing patient comfort. The breast is suspended in the imaging tank that lies below the table, through a hole in the table. The imaging tank is filled with warm, clean water. The ultrasound sensor, in the shape of a ring, surrounds the breast and moves from the chest wall to the nipple region of the breast on a motorized gantry, gathering data along the way (as shown in Figure 2).
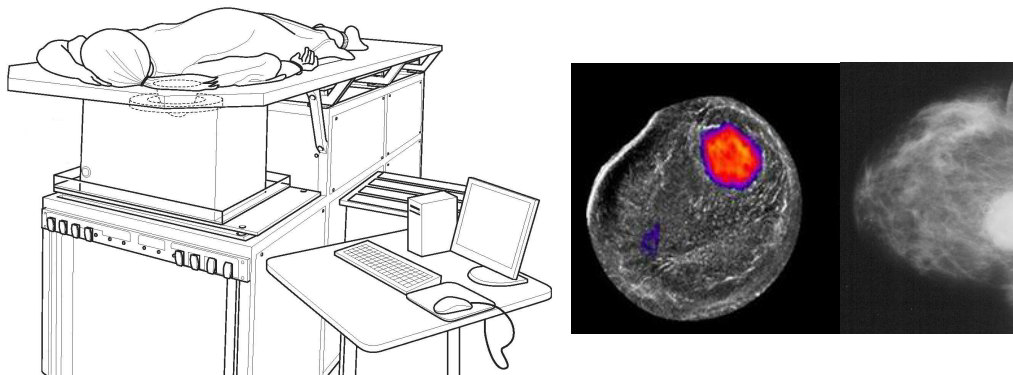

Figure 1: The UST clinical prototype (left). A patient lies in the prone position such that the breast is suspended inside a water tank that contains the ultrasound sensor. The deformable bed allows access to the chest wall as demonstrated with the images (right). (i) Cross-sectional image of the breast, with a prominent mass (in color), obtained with the UST prototype and (ii) the corresponding mammogram indicating the presence of a mass involving the chest wall.
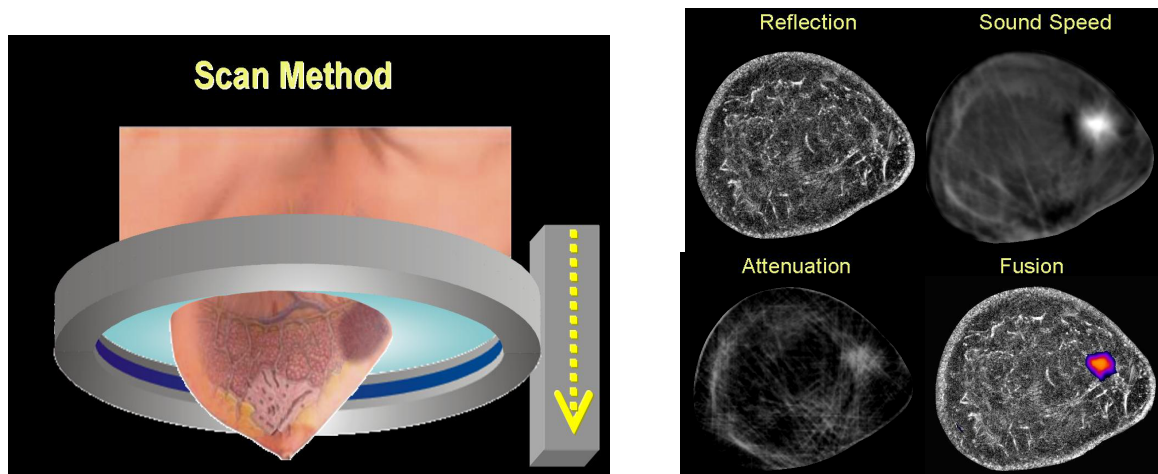

Figure 2: The ultrasound ring array (grey) surrounds the breast as it moves on a vertical trajectory from the chest wall to the nipple, acquiring data at discrete steps along the way. Each such dataset yields images of reflectivity, sound speed and attenuation, as shown. Since the images are constructed from the same data, they are intrinsically registered, allowing fast and accurate image fusion, as shown.

A total of 165 patients underwent evaluation by the latest generation ring-array transducer on the clinical US tomography prototype. Of these, 49 patients had no mass or had other miscellaneous benign masses. A total of 116 patients were diagnosed as having either a cyst, fibroadenoma (FA) or cancer, based on definitive US criteria of a cyst or biopsy confirmation. Of these, 30 were not measured because of corrupted or incomplete data during early acquisition with the new transducer version. In the final analysis, data on primary tumors from 86 patients was available.

Image Reconstruction and Analysis

Three types of images are produced from the raw data using previously described tomographic reconstruction algorithms[21,26]: (i) sound speed, (ii) attenuation and (iii) reflection. *Sound speed* images are based on the arrival times of acoustic signals. Previous studies have shown that cancerous tumors have enhanced sound speed relative to normal breast tissue[14], a characteristic which can aid the differentiation of masses, normal tissue, and fat. *Attenuation* images are tomographic reconstructions based on acoustic wave amplitude changes. Higher attenuation in cancer causes greater scatter of the ultrasound (US) wave, so attenuation data in conjunction with sound speed provides a potentially effective means for determining malignancy. *Reflection* images, derived from changes of acoustic impedance, provide echo-texture data and anatomical detail for the entire breast. Reflection images are valuable for defining tumor margins which can be used to characterize lesions through the so called Stavros criteria[11]. These 3 types of images can be combined without geometric discrepancy by means of image fusion, allowing for multi-parameter visual and quantitative characterization of masses.

A macro developed for *ImageJ* was used to fuse reflection (I_r), attenuation (I_a) and sound speed (I_s) UST images and to adjust image thresholds. Image fusion allows for improved visualization so that multiple characteristics can be viewed as one image, and breast tissue features can be evaluated more comprehensively. In addition to accentuating the lesion, the fused image depicts the local and distant tumor environment, including parenchyma and other components of breast architecture. Parenchymal tissue was visualized by varying the rendered range of sound speeds in the UST images to match the appearance of parenchyma in the MRI images. Depiction of lesions was similarly optimized using a combination of sound speed and attenuation thresholds and comparing the results with DCE-MRI renderings of the same lesions at maximum enhancement. A final fused image was created by adding the reflection image, I_r, the thresholded sound speed image, I_s, and the combined sound speed and attenuation image, I_a, as indicated by the formula,

$$ I_f = I_r + I_{s=a}^{s=b} + \left[I_{s>c} \bullet I_{a>d} \right], $$

where $\bullet$ denotes the logical .AND. operation, and *a,b,c,d* are variable threshold values.

The final image thereby displays breast architecture (via I_r), parenchyma (via I_s) and suspicious lesions (via $I_s \bullet I_a$), simultaneously. Gray-scale images, which are most comparable to MR, were used for direct visual comparison.

Mass measurements

All images were reviewed by a senior radiology resident in conjunction with a board certified radiologist having >15 years of experience in breast imaging and US-technology development. Mammographic and standard ultrasound images were only used to localize the mass, noting circumferential position (e.g. clock position) and distance from the nipple. Qualitative assessments of US tomography images were then made of the detection performance by reflection and transmission of the dominant mass. If the mass was detectable, a bimodal assessment was made whether the mass had smooth or irregular margins (1= irregular, 2 = smooth). We acknowledge that this does not include standard US BI-RADS criteria for mass evaluation and simplifies several criteria to a binary decision but similarly avoids the subjective aspects (e.g., through transmission, shadowing, etc.) that can now be quantified by sound speed and attenuation.

Quantitative values for the volume-averaged sound speed and attenuation were obtained for each mass using a 3-D region-of-interest encompassing the mass, based on threshold values that yielded mass margins most similar to those seen in MRI (as described in a previous paper[24]). The relative difference between these mass values and those of the surrounding background tissue was then quantified by subtracting the average sound speed an attenuation of the tissue surrounding the mass (defined by extending the mass ROI by 2cm).

3. RESULTS AND DISCUSSION

We have assessed the *in vivo* performance, by analyzing the reconstructed images and by tracking the data flow through the prototype system. The system's technical performance is summarized in Table 1.

Table 1. Technical performance of UST prototype.

Item	Performance
Spatial Resolution (reflection, in plane)	0.5 mm
Out-of-plane resolution	4 mm
Spatial Resolution (sound speed, in plane)	2 mm
Spatial Resolution (attenuation, in plane)	2 mm
Total patient exam time	5 min
Data throughput time	5-10 min

The clinical performance asociated with these technical figures is discussed below.

Breast Architecture:

The volumetric capability of the UST prototype is shared with MRI but not by mammography and ultrasound. We performed a small study of 22 patients to first determine whether the scanner is sensitive to similar breast structures as MRI. The initial focus of the study was to determine how reliably and accurately the breast architecture could be measured. Figure 3 illustrates a comparison of anatomy visualized by the prototype compared to that of MRI for the same patient. The enhanced MRI image (right image, fat subtracted, T1-weighted) shows the presence of fatty tissue (dark grey), parenchyma (light grey) and fibrous stroma (light bands). The corresponding ultrasound tomography image shows fatty tissue (dark) parenchyma (light grey) and fibrous stroma (white bands). During the exam, the breast is less distorted by gravity since it is surrounded by water, whereas in MRI, the breast is also pendulant but surrounded by air. Apart from these differences, these results demonstrated that the prototype can accurately map breast anatomy, thereby allowing quality control for artifacts and direct volumetric comparisons to MRI.The similarity between the MRI images and UST images may appear surprising given that MRI measures water content of tissue using magnetic resonance while UST measures biomechanical properties using acoustics. A likely explanation is that they trace similar structures because both water content and sound speed increase with tissue density[23,24,27]. The high degree of spatial correlation of MR and sound speed images is therefore largely driven by similar sensitivity to changes in tissue density.

Figure 3 (Top) UST fusion image using reflection, sound speed and attenuation data shows comparable anatomic distribution of fat, fibro-glandular tissue and fibrous bands as the MRI image **(Bottom)** from a corresponding coronal level through the breast.

Mass detection.

Although this study could not directly answer the question of whether the scanner can see masses that mammography cannot (by virtue of the pre-selection) there were a handful of cases where mammography failed to see a mass in cases where such masses were palpable (and therefore referred for biopsy) or had difficulty seeing such masses whereas the scanner could more readily detect them. Two examples are shown in Fig 4. Such findings are consistent with ultrasound's known advantages for women with dense breasts.
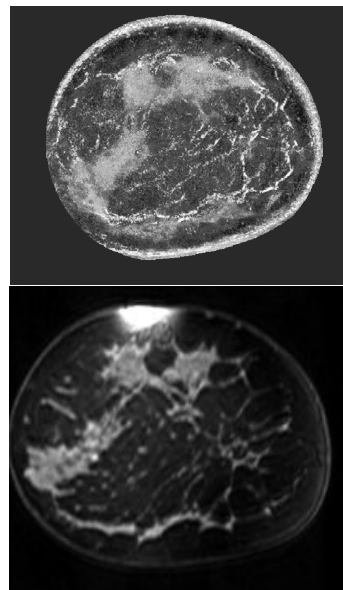
Figure 4: Top: Imaging of a 15 mm fibroadenoma: Mammogram (left) shows dense parenchyma obscuring the mass. UST reflection image: (right) shows a well circumscribed hypoechoic (dark) mass in the 2 o'clock position. Benign masses are particularly evident in our reflection images since they have more abrupt margins with adjacent tissue, whereas cancers have better conspicuity by sound speed and attenuation. **Bottom**: Imaging of a 5 mm Invasive Ductal Carcinoma: X-ray mammogram (bottom) poorly visualizes the cancer which is _not_ associated with the prominent density from scarring and prior biopsy. Fusion image from prototype data –right- combines reflection (grey scale), thresholded sound speed and attenuation to clearly identify the high sound speed and attenuation (colored region) of the small cancer at the 9:00 position.
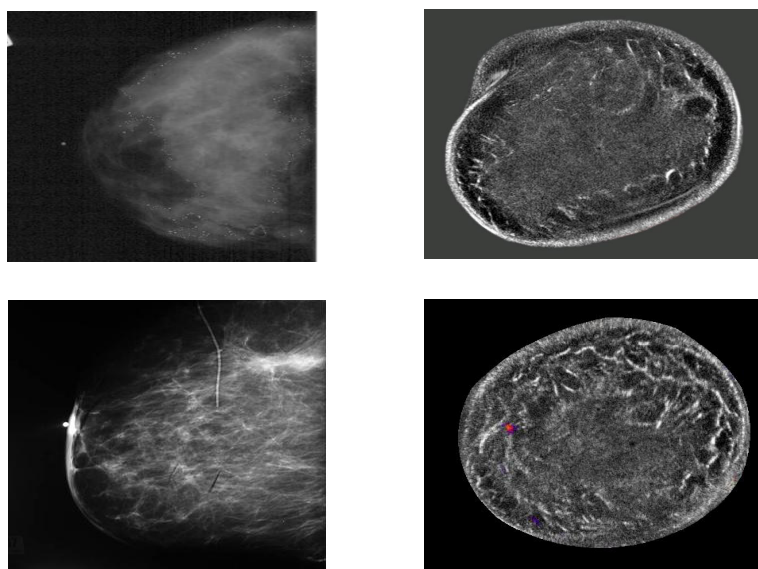
Mass characterization

Our methods exploit differences in bio-mechanical properties of tissue to differentiate various tissues and lesions in the breast. Analyses of the images, acquired in the manner described above, suggests that we can detect the variety of mass attributes noted by current ultrasound-BIRADS criteria, such as mass shape, acoustic mass properties and architecture of the tumor environment. These attributes help quantify current BIRADS criteria (e.g. "shadowing" or high attenuation) and provide greater possibilities for defining a unique signature of cancer as listed below.

1. **Irregular Margins**: Spiculated, microlobulated or ill-defined margins are more suspicious than thin and smooth margins.

2. **Architectural Distortion**: Surrounding tissue shows altered anatomy (e.g. mass effect and/or retraction).

3. **Elevated Sound Speed**: Higher sound speed than surrounding tissue is noted within the mass. Typically the sound speed is elevated by 50 to 150 m/s relative to fat.

4. **Elevated Attenuation**: Higher attenuation than surrounding tissue is noted within the mass. The amount of enhancement varies but is typically about 0.25 to 0.5 dB/cm relative to fat at 2 MHz.

Figure 4. Fusion process of UST imaging of a 15mm Invasive Ductal carcinoma. Pure reflection image (top-left) shows a hypoechoic mass at 2:00, that has high sound speed (yellow in center) and attenuation (blue). Fusion image (bottom right) shows the regions where sound speed and attenuation are both high.

The first two attributes are linked to the acoustic shape of the mass as defined by the appearance of the mass in the reflection images. They represent straightforward applications of the reflection criteria of _ultrasound-BIRADS_. The third and fourth attributes are unique to transmission ultrasound, as first defined by Greenleaf. They represent the internal acoustic properties of the mass that can be measured quantitatively in the sound speed and attenuation images. The above attributes are defined such that the probability of cancer increases with the number of attributes that are present.
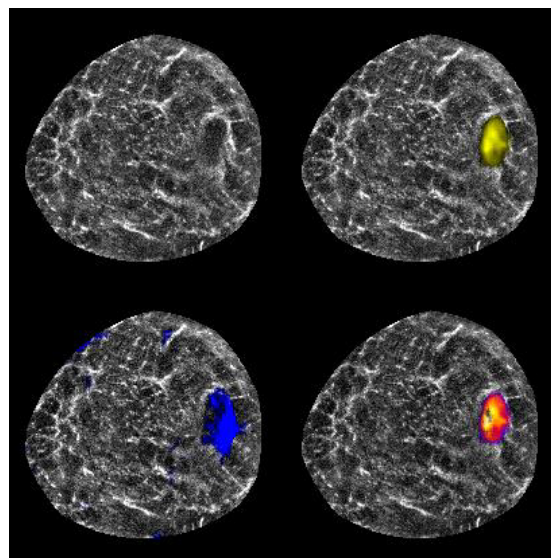
A visual example of how these attributes are utilized, is shown in Figure 5 which shows cross-sectional images from an exam of a patient diagnosed with a 15 mm cancerous mass. The reflection image on the top left shows a hypo-echoic region with, irregular margins, consistent with *ultrasound BIRADS* characterizations of cancer. Added diagnostic criteria are demonstrated in the remaining two images. The top right image was constructed by superimposing a sound speed image on the reflection image, the former thresholded at a value of 1520 m/sec. The mass clearly displays an elevated sound speed relative to a background that is almost entirely below the threshold. In the bottom left figure, an image of attenuation, thresholded at a value of 0.20 dB/cm, is shown superimposed on the reflection image. The fused image, shown in the bottom right, was created with a Boolean AND operation showing only those regions where both the sound speed *and* the attenuation exceed their thresholds. It shows that the sound speed and attenuation are both elevated, indicators of cancer according to the *Greenleaf* criteria.

The above mass attributes were determined for each mass in our sample. These properties were then used to predict whether lesions were cancer or benign by varying cut-points associated with combinations of these properties. A scatter plot visualizing the distribution of mass characteristics is shown in Figure 5. If the cut-point line is moved to achieve 100% sensitivity, the positive predictive value (PPV) is 82% with a specificity of 81% (38/47) and negative predictive value (NPV) of 100% (38/38). In the case of conventional US, assuming 100% sensitivity, or all solid masses undergoing biopsy and only cysts considered negative, PPV is 53% (39/73), specificity only 28% (13/47) and NPV is 100% (13/13).
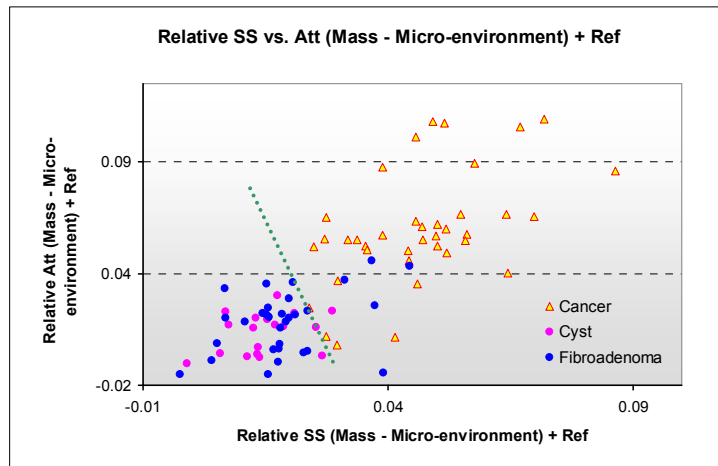
4. CONCLUSIONS

Analysis of clinical breast images reconstructed from simultaneous acquisitions of reflection and transmission UST data are presented. These results indicate that operator-independent whole-breast imaging and the detection of cancerous breast masses are feasible using ultrasound tomography techniques. The combination of these images reveals major breast anatomy, including fat, parenchyma, fibrous stroma and masses. Analysis of the prototype images suggests that we can detect the variety of mass attributes noted by current ultrasound-BIRADS criteria, such as mass shape, acoustic mass properties and architecture of the tumor environment. These attributes help quantify current BIRADS criteria (e.g. "shadowing" or high attenuation) and provide greater possibilities for defining a unique signature of cancer.

Fusion imaging, utilizing thresholding, is shown to visualize mass characterization and facilitates separation of cancer from benign masses. These results indicate that operator-independent whole-breast imaging and the detection and characterization of cancerous breast masses are feasible using acoustic tomography techniques. The potential for UST to detect and characterize breast masses was quantified using UST measurements of 86 masses from the most recent cohort of patients imaged with the latest version of our prototype. Our results suggest that the development of a formal predictive model, in support of larger future trials, is warranted.

5. ACKNOWLEDGMENTS

6. REFERENCES

[1] Berry DA, et al., Effect of Screening and Adjuvant Therapy on Mortality from Breast Cancer. N Engl J Med. 2005; 1784-1792

[2] Gotzsche PC, Olsen O. Is screening for breast cancer with mammography justifiable? Lancet 2000; 355:129–134.

[3] van den Biggelaar FJ, Nelemans PJ, Flobbe K. Performance of radiographers in mammogram interpretation: a systematic review. Breast. 2008; 17:85-90.

[4] Schell MJ, Yankaskas BC, Ballard-Barbash R, Qaqish BF, Barlow WE, Rosenberg RD, Smith-Bindman R. Evidence-based target recall rates for screening mammography. Radiology. 2007; 243:681-9.

[5] Armstrong K, Moye E, Williams S, Berlin JA, Reynolds EE. Screening mammography in women 40 to 49 years of age: a systematic review for the American College of Physicians. Ann Intern Med. 2007; 146:516-26

[6] Kuhl CK, Schrading S, Bieling HB, Wardelmann E, Leutner CC, Koenig R, Kuhn W, Schild HH. MRI for diagnosis of pure ductal carcinoma in situ: a prospective observational study. Lancet. 2007; 370:485-92.

[7] Saslow D, Boetes C, Burke W, Harms S, Leach MO, Lehman CD, Morris E, Pisano E, Schnall M, Sener S, Smith RA, Warner E, Yaffe M, Andrews KS, Russell CA; American Cancer Society Breast Cancer Advisory Group. American Cancer Society guidelines for breast screening with MRI as an adjunct to mammography. CA Cancer J Clin. 2007; 57:75-89.

[8] Kolb, T.M., Lichy, J. and Newhouse, J.H. Comparison of the Performance of Screening Mammography, Physical Examination, and Breast US and Evaluation of Factors that Influence Them: An Analysis of 27,825 Patient Evaluation. Radiology, 2002; 225: 165-175.

[9] ACRIN website: www.acrin.org .

[10] Berg WA, Blume JD, Cormack JB, Mendelson EB, Lehrer D, Böhm-Vélez M, Pisano ED, Jong RA, Evans WP, Morton MJ, Mahoney MC, Hovanessian Larsen L, Barr RG, Farria DM, Marques HS, Boparai K, for the ACRIN 6666 Investigators. Combined Screening With Ultrasound and Mammography vs Mammography Alone in Women at Elevated Risk of Breast Cancer. JAMA 2008;299(18):2151-2163.

[11] Stavros AT, Thickman D, Rapp CL, Dennis MA, Parker SH, Sisney GA. Solid breast nodules: use of sonography to distinguish between benign and malignant lesions. Radiology. 196:123-34, 1995.

[12] Norton SJ, Linzer M. Ultrasonic reflectivity tomography: reconstruction with circular transducer arrays. Ultrason Imaging 1979. Apr;1(2):154-84.

[13] http://www.u-sys.com/

[14] Greenleaf JF, Johnson SA, Bahn RC, Rajagopalan B: *Quantitative cross-sectional imaging of ultrasound parameters.* 1977 Ultrasonics Symposium Proc., 1977, IEEE Cat. # 77CH1264-1SU, pp. 989- 995.

[15] Carson PL, Meyer CR, Scherzinger AL, Oughton TV. Breast imaging in coronal planes with simultaneous pulse echo and transmission ultrasound. Science 1981, Dec 4;214(4525):1141-3.

[16] Andre MP, Janee HS, Martin PJ, Otto GP, Spivey BA, Palmer DA, "High-speed data acquisition in a diffraction tomography system employing large-scale toroidal arrays," International Journal of Imaging Systems and Technology 1997;Vol. 8, Issue 1:137-147.

[17] Johnson SA, Borup DT, Wiskin JW, Natterer F, Wuebbling F, Zhang Y, Olsen C. *Apparatus and Method for Imaging with Wavefields using Inverse Scattering Techniques*. United States Patent 6,005,916 (1999).

[18] Marmarelis VZ, Kim T, Shehada RE. Proceedings of the SPIE: Medical Imaging; Ultrasonic Imaging and Signal Processing 2003, Paper 5035-6.

[19] Liu D-L, Waag RC. "Propagation and backpropagation for ultrasonic wavefront design," *IEEE Trans. on Ultras. Ferro. and Freq. Contr*. 1997;44(1):1-13.

[20] Duric N, Littrup PJ, Babkin A, Chambers D, Azevedo S, Kalinin A, Pevzner R, Tokarev M, Holsapple E, Rama O,

Duncan R. Development of Ultrasound Tomography for Breast Imaging: Technical Assessment. Medical Physics. May 2005, Vol. 32, No. 5, pp. 1375–1386.

[21] Duric N, Littrup P, Poulo L, Babkin A, Pevzner R, Holsapple E, Rama O, Glide C. Detection of Breast Cancer With Ultrasound Tomography: First Results with the Computerized Ultrasound Risk Evaluation (C.U.R.E) Prototype. Medical Physics Feb 2007; Vol 34 (2), pp. 773-785.

[22] Glide CK, Duric N. Littrup P. A new method for quantitative analysis of mammographic density. Med Phys. 2007 Nov; Vol. 34, Issue 11:4491-4498.

[23] Glide-Hurst C, Duric N, Littrup P. Volumetric breast density evaluation from ultrasound tomography images. Med Phys. 2008;Vol. 35, Issue 9, pp. 3988-3997.

[24] Duric N, Li C, Littrup PJ, Huang L, Glide-Hurst C, Rama O, Bey-Knight L, Schmidt S, Xu Y, Lupinacci J. Detection and characterization of breast masses with ultrasound tomography: clinical results. Proc. SPIE 2008; 6920, 6920-28.

[25] Lupinacci J, Duric N, Li C, Littrup P, Wang D, Rama O, Schmidt S. Monitoring of breast masses with ultrasound tomography for patients undergoing neoadjuvant chemotherapy. Proc. SPIE 2009;7265, 7265-43.

[26] Li C, Duric N, Huang L. Clinical breast imaging using sound-speed reconstructions of ultrasound tomography data. Proc. SPIE 2008;6920, 6920-09.

[27] Boyd, N.F., et al., *Breast-tissue composition and other risk factors for breast cancer in young women: a cross-sectional study.* Lancet Onc. 2009. 10(6): pp.569-580.